Superplastic behaviour of rapidly solidified ultrahigh carbon alloy tool steel X380 CrVMo 25 9 3

H. J. Speis and G. Frommeyer

This paper describes the superplastic properties of the rapidly solidified (RS) ultrahigh carbon alloy tool steel X380 CrVMo 25 9 3. By application of a specific production route, a microcrystalline structure can be produced which consists of a ferritic matrix (grain size $d \leqslant 3{\cdot}8$ μm) and fine dispersed carbides ($d = 1$–3 μm). At test temperatures T of about 1050°C the tool steel can be deformed superplastically. Maximum tensile elongations are limited by cavity formation at the austenite/carbide interfaces. Compression tests reveal clearly that the cavity volume is decreased compared with that found in tensile tests. The mechanism for accommodation of grain boundary sliding is discussed in the light of scanning electron microscopy (SEM) and transmission electron microscopy (TEM) investigations. To demonstrate the potential of the tool steel X370 CrVMo 25 9 3 for the production of near net shape components some samples were precision forged in the superplastic regime. MST/1378

 Manuscript received 7 November 1990; in final form 17 April 1991. *The authors are in the Department of Materials Technologies, Max-Planck-Institut für Eisenforschung GmbH, Düsseldorf, Germany.*

Introduction

Rapid solidification (RS) techniques, especially gas atomisation, provide a unique possibility of producing new alloys, including ultrahigh carbon alloy tool steels, which cannot be manufactured by conventional melting, casting, and hot working processes.[1–3] For example, segregation of primary carbides during conventional processing leads to non-uniform distributions of these carbides even after substantial amounts of hot deformation. As a result of their inhomogeneous microstructures these tool steels show non-uniform hardness and variations in grinding behaviour and wear resistance.[3,4]

In contrast, the microstructures of powder metallurgically processed tool steels consist of a fine and uniform distribution of carbides within the matrix, resulting in excellent isotropic properties.

Unfortunately, the recently developed high alloy tool steels show poor machinibility owing to the large volume fraction of hard special carbides. To overcome these problems one of the important aims of current research is to produce near net shape parts by superplastic forming technology such as press forging of bulk materials into dies.[5]

Structural superplasticity is the ability, under certain deformation conditions, of fine grained and equiaxed polycrystalline materials to show large plastic elongations without necking.[6,7] Superplasticity in metallic materials has been reviewed extensively, and many investigations have been carried out on the superplastic properties of aluminium, titanium, nickel, and iron base alloys.[6–10] However, until now no work has been published which considers the superplastic behaviour of ultrahigh carbon alloy tool steels. This is owing to the high volume fraction of special carbides, e.g. VC and Cr_7C_3, which have considerably higher hardness and flow stress compared with the softer ferritic or austenitic matrix. This will lead to premature failure during superplastic straining as a consequence of cavity formation at the interfaces.[11–13]

The present paper describes the superplastic behaviour of a powder metallurgically processed ultrahigh carbon alloy tool steel, with a view to superplastic precision forming of bulk parts of complex shape.

Experimental

To obtain a fine distribution of second phase particles, the tool steel was prepared by melt atomisation using a nitrogen gas jet. The cooling rate of the powder particles depends upon their size and was estimated from secondary dendritic arm spacings to be $\dot{T} = 10^3$–10^5 K s^{-1} (Ref. 14). For the manufacture of bulk specimens, the powder was encapsulated in a mild steel can and, after degassing, was compacted by hot extrusion at $T = 1150$°C to produce rods with about 84% reduction in cross-section.

The nominal chemical composition of the consolidated material (designation X380 CrVMo 25 9 3) is given in Table 1.

Flat tensile specimens of 3·5 mm thickness, 5 mm width, and 15 mm gauge length were machined by spark erosion from the consolidated material. To investigate the superplastic behaviour of the material tensile tests were carried out in the temperature range $T = 750$–1100°C using a Zwick 1474 tensile testing machine at constant crosshead speed. Strain rate change tests were performed to determine the strain rate sensitivity parameter as well as the stress–strain relationship. The parameter m is a measure of the strain rate sensitivity of the flow stress at constant temperature and microstructure. Superplasticity in materials occurs when strain rate sensitivity is of the order of $m \geqslant 0{\cdot}3$.

Elongation to failure was measured to determine the tensile ductility at the strain rates for which the tool steel shows highest strain rate sensitivity.

In addition, some compression tests were carried out to investigate the dependence of cavity volume on deformation direction.

Microstructural characterisation, i.e. grain size of the matrix and volume fraction, distribution, and particle size of the second phase, was carried out by light optical and scanning electron (SEM) microscopy. Transmission electron microscopy (TEM) was used to determine the difference in the microstructures of the undeformed and superplastically deformed specimens.

Results

MICROSTRUCTURE OF CONSOLIDATED TOOL STEEL

Typical microstructures of the hot extruded rods are shown in Figs. 1*a* and 1*b*. It can be seen that hot extrusion of the

Table 1 Nominal composition of steel used, wt-%

C	Si	Mn	Cr	Mo	V	Fe
3·8	0·6	0·6	24·9	2·7	8·7	Bal.

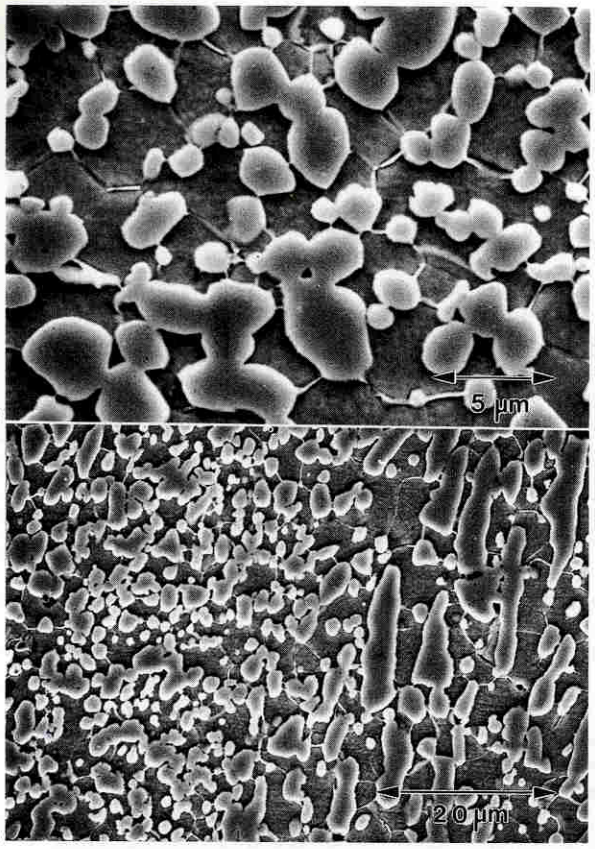

a homogeneous distribution of carbides in matrix (cross-section); *b* elongated carbide stringers and coalescence of carbides (longitudinal section)

1 Microstructure of consolidated tool steel (SEM)

powder yields a dense and equiaxed microstructure. The grain size (mean linear intercept) of the ferritic matrix is of the order of 3·8 μm. The micrographs reveal a bimodal distribution of the carbides. These have been identified by energy dispersive spectroscopy (EDS) in the SEM; the larger precipitates are chromium rich $M_{23}C_6$ (M = Cr, Fe, V) carbides 1·5–3 μm in size, whereas the smaller are iron rich carbides approximately 1 μm in size. Because of the large carbide volume fraction of about 43 vol.-%, coalescence occurred during hot extrusion (Fig. 1*b*). Some elongated carbide stringers up to 20 μm in length (aspect ratio $l/d = 6$) and aligned parallel to the extrusion direction are also shown in Fig. 1*b*.

STRESS–STRAIN RATE RELATIONSHIP

The superplastic behaviour of the compacted tool steel was studied in strain rate change tests performed in the

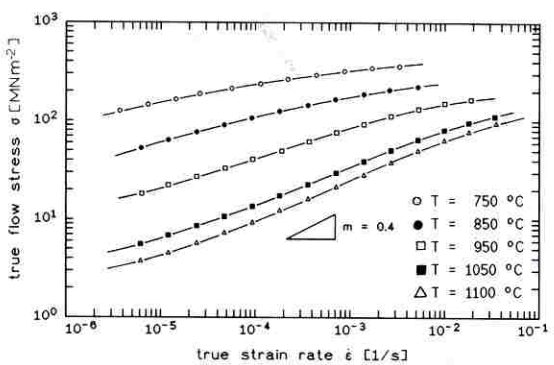

2 True flow stress σ as function of true strain rate $\dot{\varepsilon}$ for different test temperatures

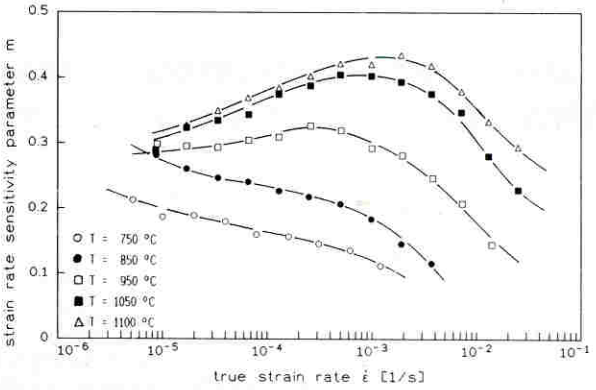

3 Strain rate sensitivity parameter m as function of strain rate $\dot{\varepsilon}$ for different temperatures

temperature range $750 \leqslant T \leqslant 1100°C$. The results are shown in Fig. 2 in the form of a double logarithmic plot of true flow stress σ as a function of true strain rate $\dot{\varepsilon}$. To determine the strain rates for which the flow stress of the tool steel shows the highest strain rate sensitivity, m is calculated using the equation

$$m = \frac{\log(\sigma_1/\sigma_2)}{\log(\dot{\varepsilon}_1/\dot{\varepsilon}_2)} \quad \ldots\ldots\ldots\ldots\ldots\ldots \quad (1)$$

The values of m obtained are in the range $0{\cdot}3 \leqslant m \leqslant 0{\cdot}4$, and tend to increase with increasing test temperature (Fig. 3). The optimum superplastic deformation temperature lies in the range $T = 1050 \pm 50°C$ with a maximum value of $m = 0{\cdot}44$ at a strain rate of $\dot{\varepsilon} = 1 \times 10^{-3}\ s^{-1}$.

The activation energy Q for superplastic deformation was calculated using the equation[15]

$$Q = -R\left.\frac{\mathrm{d}(\ln\dot{\varepsilon})}{\mathrm{d}(1/T)}\right|_{\sigma} \quad \ldots\ldots\ldots\ldots\ldots\ldots \quad (2)$$

where T is the absolute test temperature and R is the gas constant. The calculation was carried out for superplastic tests performed in the temperature range $975 \leqslant T \leqslant 1075°C$ at three constant flow stresses. The activation energy for superplastic flow in this region was determined to be $Q = 298 \pm 5\ kJ\ mol^{-1}$ (*see* Fig. 4).

TENSILE DUCTILITY

The tensile ductility of the tool steel samples was measured for optimised superplastic deformation parameters m and T at constant crosshead speed. At the test temperatures of

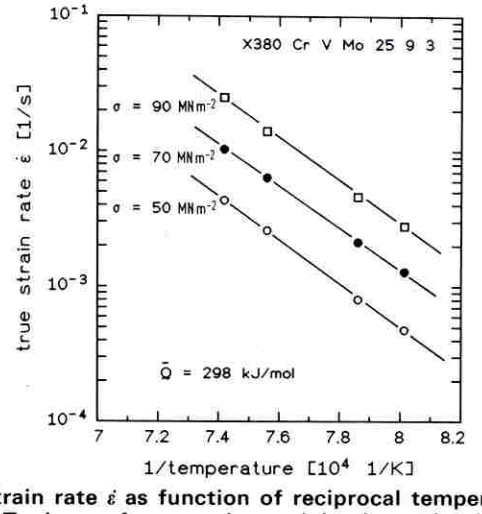

4 Strain rate $\dot{\varepsilon}$ as function of reciprocal temperature $1/T$: slope of curves is used in determination of activation energy for superplastic deformation

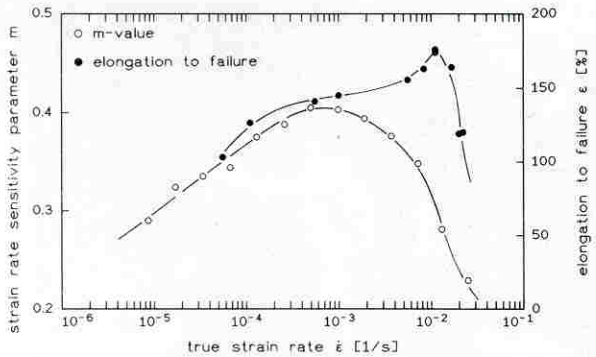

5 Elongation to failure and m as functions of true strain rate $\dot{\varepsilon}$

$T = 1000$ and 1050°C maximum elongations of 150% and 176% respectively were obtained. Figure 5 shows total elongation and m as functions of true strain rate. The maximum of the elongation curve is shifted to higher true strain rates compared with the m versus strain rate curve.

MICROSTRUCTURES AFTER TENSILE DEFORMATION

Investigations using SEM and TEM on superplastically deformed samples show that some grain growth occurred during superplastic flow.

Figure 6 shows typical microstructures of the deformed region in two samples after superplastic elongation at $T = 1050$°C with different initial strain rates.

The size and shape of the grains depend upon the strain rates at which the tests were carried out. Figure 6*a* shows

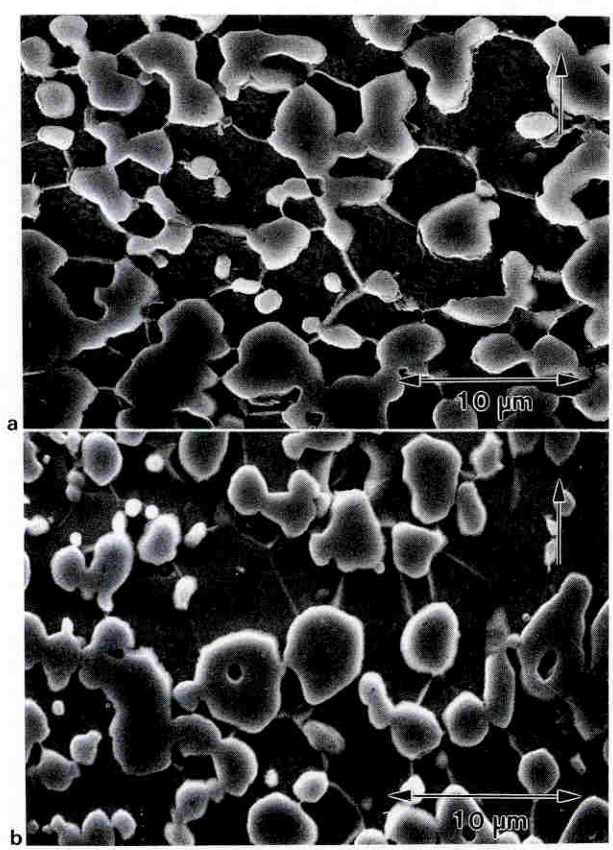

a equiaxed grains, $\dot{\varepsilon} = 6 \times 10^{-4}\,s^{-1}$; *b* elongated grains, $\dot{\varepsilon} = 1{\cdot}1 \times 10^{-2}\,s^{-1}$

6 Typical microstructures of two tensile test samples deformed at $T = 1050$°C (SEM)

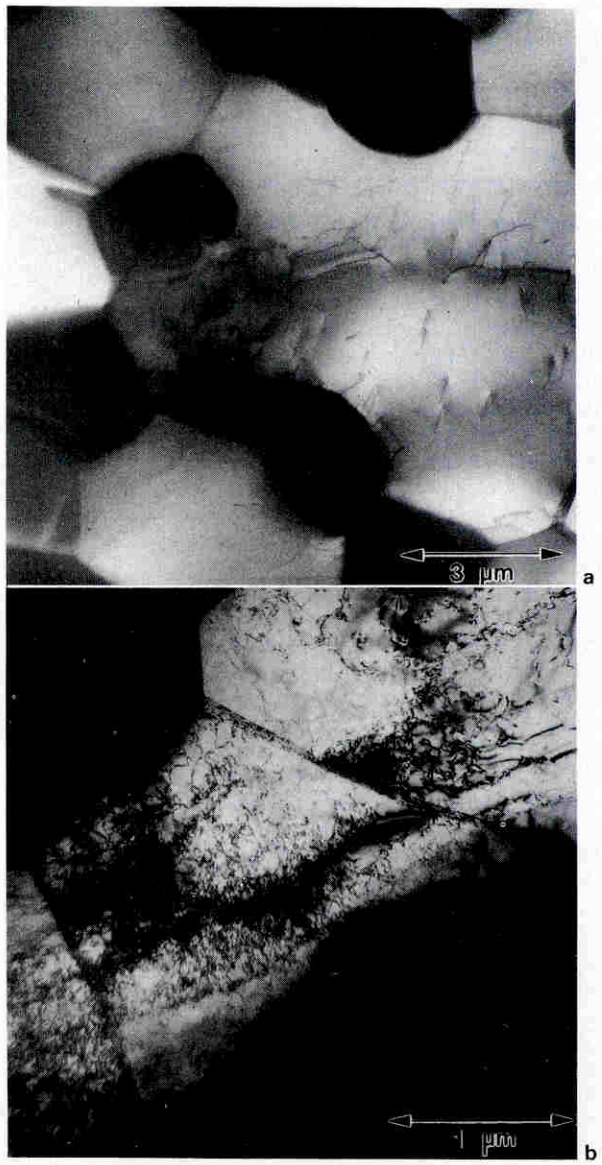

a low dislocation density, $\dot{\varepsilon} = 6 \times 10^{-4}\,s^{-1}$; *b* higher dislocation density, $\dot{\varepsilon} = 1{\cdot}1 \times 10^{-2}\,s^{-1}$

7 Strained region of two superplastically deformed samples corresponding to Figs. 6*a* and 6*b* (TEM)

the microstructure of a tensile test sample which was deformed with an initial strain rate $\dot{\varepsilon} = 6 \times 10^{-4}\,s^{-1}$, which corresponds to the maximum in m (*see* Fig. 3). It can be seen that after superplastic deformation the shape of the grains remained equiaxed but some grain growth occurred. The matrix grain size in the undeformed and in the superplastically deformed state was found to be 5·4 µm. In contrast, the grain size of samples deformed with a higher initial strain rate of $\dot{\varepsilon} = 1{\cdot}1 \times 10^{-2}\,s^{-1}$ to a total elongation of 170% was somewhat smaller ($d = 4{\cdot}1$ µm) owing to the shorter test time. Furthermore, Fig. 6*b* reveals that the grains are slightly elongated in the deformation direction.

In Figs. 7*a* and 7*b*, TEM images from samples corresponding to Figs. 6*a* and 6*b* are shown. Figure 7*a* reveals that the grains of the sample (Fig. 6*a*) remain equiaxed. Furthermore, although a few dislocation tangles are present in some grains, most grains are dislocation free. There was no increase in dislocation density in comparison with the undeformed region of the same sample.

In contrast to this the grains of the second sample, corresponding to Fig. 6*b*, show a higher defect density consisting of dislocations and low angle grain boundaries

(*see* Fig. 7*b*) which lead to the conclusion that accommodated slip occurs during superplastic deformation of this sample.

Discussion

Investigations using SEM (*see* Fig. 1) reveal clearly that gas atomisation and rapid solidification is a successful method for the production of ultrahigh carbon alloy tool steel powders. Because of the fine grained microstructure, which consists of uniformly distributed carbides within a ferritic α matrix having an average grain size of 3·8 μm, the tool steel exhibits superplasticity. Optimum superplastic properties have been observed in the temperature range $1000 \leqslant T \leqslant 1100°C$ at m values of about 0·4 and strain rates of the order of $\dot{\varepsilon} = 1 \times 10^{-3}\,s^{-1}$. The maximum elongation to failure ε of 170% is limited by cavity formation at the carbide/matrix interfaces, as shown in Fig. 8. Preferential cavity formation at the interphase boundaries reflects the inability of the carbide phases to make a significant contribution to the accommodation of grain boundary sliding by either dislocation or diffusion processes. Because of the large carbide volume fraction of 43 vol.-% the grain boundaries in the X380 CrVMo 25 9 3 tool steel consist of high angle grain boundaries in the austenitic γ matrix and carbide/austenitic phase boundaries. During superplastic straining the dominant deformation mechanism of the investigated tool steel can be described as a combination of grain and interphase boundary sliding. Since the hard carbides do not deform, cavities will be formed at the matrix/carbide interfaces.[16] During straining the cavities grow and early fracture of the sample is caused by the interlinking of cavities. This can clearly be seen in the SEM in Fig. 9, which shows a fracture surface of a superplastically deformed sample, where the fracture is initiated by the coalescence of cavities to form pores with sizes up to 20 μm. Furthermore, these cavities will be formed preferentially in the regions where elongated carbide stringers are present. This is due to the incomplete accommodation mechanism which is unable to reduce internal stresses by diffusion mechanisms.

Assuming a homogeneous microstructure, it might be possible to increase the ductility in tension. Since cavitation leads to degradation of service properties,[17] it is necessary to suppress cavity formation during superplastic deformation. A change in the deformation mode from tension to compression reduces the total volume fraction of cavities, as can be seen in Fig. 10. A further reduction of the cavity volume is caused by an increase of the diameter/height (D/H) ratio of cylindrical compression specimens, as shown in Fig. 10.[18] Investigations using SEM on deformed compression specimens revealed that the cavities were formed preferentially in the barrelled regions of the specimens. Increasing the D/H ratio decreases the barrelling tendency and the amount of material subjected to circumferential tensile stresses.

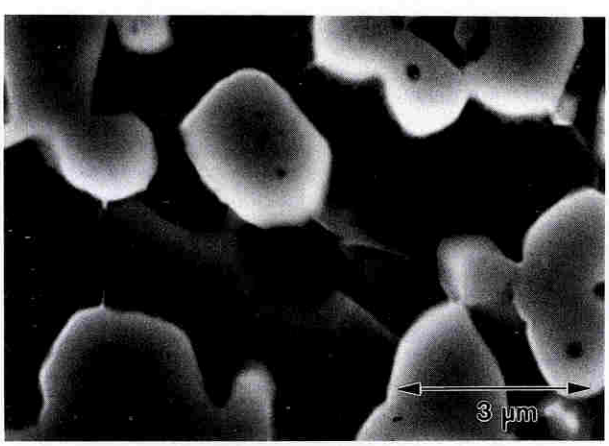

8 Cavity formation at carbide/matrix interfaces (SEM)

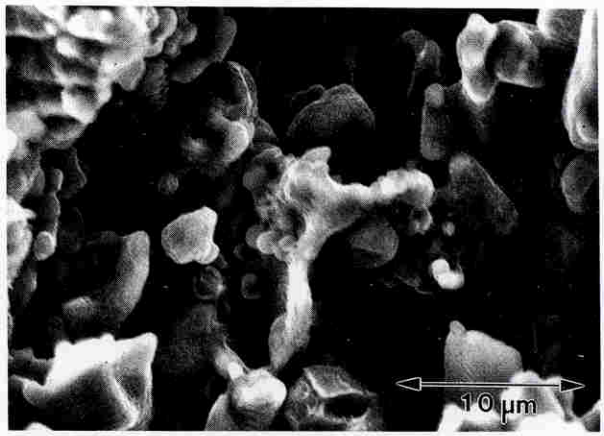

9 Fracture surface of test sample superplastically deformed at $T = 1050°C$ and $\dot{\varepsilon} = 6 \times 10^{-4}\,s^{-1}$ to total elongation $\varepsilon = 150\%$ (SEM)

In contrast to other superplastic ferrous and non-ferrous alloys the maximum elongations obtained do not coincide with the maximum m value (Ref. 13). The largest elongations were detected at higher strain rates and lower values of m. This implies that a transition takes place from the superplastic region where grain boundary sliding occurs to the region where slip controls the deformation.[13] Slip is a dominant deformation mechanism at higher strain rates ($\dot{\varepsilon} \geqslant 10^{-2}\,s^{-1}$), as can be demonstrated by microstructural investigations. The SEM in Fig. 6*b* clearly reveals elongated grains, parallel to the tensile direction, which are caused by glide inside the grains. This is accompanied by dislocation movement, as can be seen in the TEM in Fig. 7*b*.

Taking normal grain growth into account, the amount of slip estimated from the elongated grains in the deformation direction accounts for about 20% of the total elongation. This implies that grain elongation by slip deformation must be subtracted from the total tensile ductility. Therefore, it follows that the largest elongation will be found in the strain rate region showing maximum m.

Normally, the internal tensile stresses which arise at the interfaces during superplastic deformation will be reduced

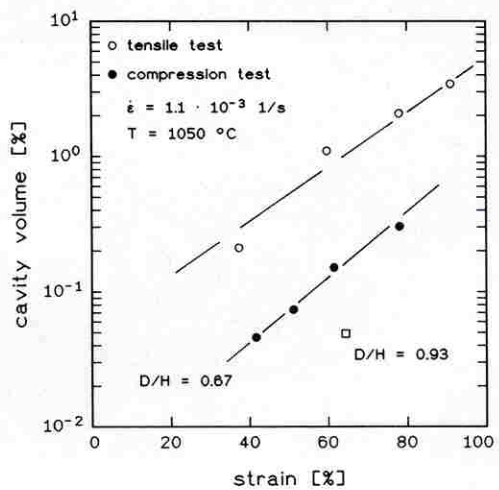

10 Comparison of amount of cavitation in tool steel deformed superplastically in tension and in compression

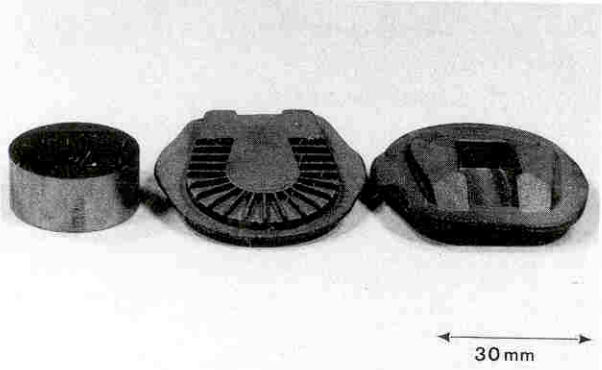

11 Superplastic precision forging of tool steel X380 CrVMo 25 9 3 at $T = 1050°C$, $\dot{\varepsilon} = 5 \times 10^{-2} s^{-1}$ (Courtesy of Sulzer Innotec, Winterthur, Switzerland)

by diffusion.[8,11] Because of the larger carbides grain accommodation by diffusion and slip at matrix/carbide interfaces will be hindered and consequently more cavities will be formed at the interfaces. This leads to preferential fracture of the test samples deformed in tension. When slip deformation acts as an accommodation mechanism the internal tensile stresses are reduced by dislocation glide, and it is possible to achieve a greater elongation compared with deformation in the strain rate region where grain or phase boundary sliding are accommodated by diffusion.

As mentioned above, the activation energy was determined to be $Q = 298 \pm 5$ kJ mol^{-1}. From this value of Q, an attempt can be made[19] to identify the governing accommodation mechanisms, e.g. lattice or grain boundary diffusion. The calculated activation energy of $Q = 298$ kJ mol^{-1} is higher than the activation energies[20] for grain boundary diffusion of iron in pure γ iron ($Q_{GB} = 170$ kJ mol^{-1}) and for lattice self-diffusion ($Q_V = 280$ kJ mol^{-1}). Owing to the extremely high alloying content of the tool steel, these values are not comparable to the activation energies for lattice diffusion in the solid solution matrix or for grain or interphase boundary diffusion. It is worthy of note that no diffusion data for such a complex system have yet been published.

An investigation of superplastic ceramics[21] has shown that the activation energy for grain boundary sliding in the superplastic regime is raised by a factor of 1·66 when an insoluble hard second phase is alloyed with the softer matrix.

From a consideration of these results, grain or interphase boundary diffusion might act as the dominant accommodation mechanism during superplastic deformation of this type of high alloy steel.

To evaluate the near net shape forming potential of the investigated tool steel, some superplastic precision forging tests were carried out. Samples of the tool steel were superplastically deformed at $T = 1050°C$ in a protective atmosphere using an isothermal forging machine. Figure 11 demonstrates the extraordinary near net shape potential of the tool steel X380 CrVMo 25 9 3.

Conclusions

1. Melt atomisation and subsequent hot extrusion is a useful method for the successful production of high alloy tool steel consisting of a two phase microcrystalline structure.

2. The tool steel X380 CrVMo 25 9 3 exhibits superplasticity in the temperature range $T = 1050 \pm 50°C$.

3. The tensile ductility $\varepsilon \leqslant 170\%$ is limited by cavity formation at the interphase boundaries.

4. Grain boundary sliding, which is the dominant deformation mechanism during superplastic straining, is accommodated by grain boundary diffusion.

Acknowledgment

The financial support of this work by the Ministry for Economic Affairs and Technology for North Rhine–Westphalia is gratefully acknowledged.

References

1. E. J. DULIS and T. A. NEUMEYER: in 'Modern developments in powder metallurgy', (ed. P. U. Gummeson and D. A. Gustafson), Vol. 20, 129–142; 1988, London, Plenum Press.
2. P. HELLMAN, H. LARKER, J. B. PFEFFER, and I. STROMBLAD: in 'Modern developments in powder metallurgy', (ed. P. U. Gummeson and D. A. Gustafson), Vol. 4, 573–582; 1970, London, Plenum Press.
3. B. HRIBERNIK and M. GSTETTNER: *Steel Res.*, 1985, **56**, 225–228.
4. E. HABERLING: *Stahl Eisen*, 1975, **94**, (10), 454–462.
5. O. D. SHERBY and J. WADSWORTH: *Prog. Mater. Sci.*, 1989, **33**, 169–221.
6. In Proc. Conf. 'Superplasticity and superplastic forming', (ed. C. H. Hamilton and N. E. Paton); 1988, Warrendale, PA, TMS.
7. K. A. PADMANABHAN and G. J. DAVIES: 'Superplasticity'; 1980, Berlin/ Heidelberg/New York, Springer-Verlag.
8. O. D. SHERBY, B. WALSER, C. M. YOUNG, and E. M. CADY: *Scr. Metall.*, 1975, **9**, 569–574.
9. D. W. KUM, G. FROMMEYER, N. J. GRANT, and O. D. SHERBY: *Metall. Trans.*, 1987, **18A**, 1703–1711.
10. N. RIDLEY: in Proc. Conf. 'Superplastic forming of structural alloys', (ed. N. E. Paton and C. H. Hamilton), 191–207; 1982, Warrendale, PA, The Metallurgical Society of AIME.
11. R. PEARCE: *AGARD Rep.*, 1987, (154), Paper 1.
12. M. J. STOWELL: in Proc. Conf. 'Superplastic forming of structural alloys', (ed. N. E. Paton and C. H. Hamilton), 321–336; 1982, Warrendale, PA, The Metallurgical Society of AIME.
13. J. W. EDINGTON, K. MELTON, and C. P. CUTLER: *Prog. Mater. Sci.*, 1976, **21**, 61–170.
14. G. FROMMEYER: in Proc. 'Seminar on rapid solidification', 1–55; 1989, Dresden, Zentralinstitut für Festkörperphysik und Werkstoffforschung, Akademie der Wissenschaften.
15. F. A. MOHAMED and T. G. LANGDON: *Phys. Status Solidi (a)*, 1976, **33**, 375–381.
16. N. RIDLEY: in *AGARD Rep.*, 1987, (154), Paper 4.
17. C. C. BAMPTON and J. W. EDINGTON: *J. Eng. Mater. Technol., (Trans. ASME)*, 1983, **105**, 55–60.
18. D. W. LIVESEY and N. RIDLEY: *Met. Sci.*, 1982, **16**, 563–568.
19. O. D. SHERBY and J. WADSWORTH: in 'Deformation, processing and structure', (ed. G. Kraus), 355–388; 1984, Metals Park, OH, ASM.
20. 'Handbook of grain and interphase boundary diffusion data', (ed. I. Kaur and W. Gust), Vol. 1; 1989, Stuttgart, Ziegler Press.
21. I.-W. CHEN and L. A. XUE: *J. Am. Ceram. Soc.*, 1990, **73**, (9) 2585–2609.